We are IntechOpen, the world's leading publisher of Open Access books Built by scientists, for scientists

5,300
Open access books available

130,000
International authors and editors

155M
Downloads

Our authors are among the

154
Countries delivered to

TOP 1%
most cited scientists

12.2%
Contributors from top 500 universities

CLARIVATE ANALYTICS
BOOK CITATION INDEX
INDEXED

WEB OF SCIENCE™

Selection of our books indexed in the Book Citation Index
in Web of Science™ Core Collection (BKCI)

Interested in publishing with us?
Contact book.department@intechopen.com

Localization of Buried Objects in Sediment Using High Resolution Array Processing Methods

Caroline Fossati, Salah Bourennane and Julien Marot
Institut Fresnel, Ecole Centrale Marseille
France

1. Introduction

Non-invasive range and bearing estimation of buried objects, in the underwater acoustic environment, has received considerable attention (Granara et al., 1998).

Many studies have been recently developed. Some of them use acoustic scattering to localize objects by analyzing acoustic resonance in the time-frequency domain, but these processes are usually limited to simple shaped objects (Nicq & Brussieux, 1998). In (Guillermin et al., 2000) the inversion of measured scattered acoustical waves is used to image buried object, but the frequencies used are high and the application in a real environment should be difficult. The acoustic imagery technique uses high frequencies that are too strongly attenuated inside the sediment therefore it is not suitable. Another method which uses a low frequency synthetic aperture sonar (SAS) has been applied on partially and shallowly buried cylinders in a sandy seabed (Hetet et al., 2004). Other techniques based on signal processing such as time reversal technic (Roux & Fink, 2000), have been also developed for object detection and localization but their applicability in real life has been proven only on cylinders oriented in certain ways and point scatterers. Furthermore, having techniques that operate well for simultaneous range and bearing estimation using wideband and fully correlated signals scattered from nearfield and farfield objects, in a noisy environment, remains a challenging problem.

In this chapter, the proposed method is based on array processing methods combined with an acoustic scattering model. Array processing techniques, as the MUSIC method, have been widely used for acoustic point sources localization. Typically these techniques assume that the point sources are on the seabed and are in the farfield of the array so that the measured wavefronts are all planar. The goal then is to determine the direction of arrival (bearing) of these wavefronts. These techniques have not been used for bearing and range estimation of buried objects and in this chapter we are interested to extend them to this problem. This extension is a challenging problem because here the objects are not point sources, are buried in the seabed and can be everywhere (in the farfield or in the nearfield array). Thus the knowledge of the bearing is not sufficient to localize the buried object. Furthermore, the signals are correlated and the Gaussian noise should be taken into account. In addition we consider that the objects have known shapes. The principal parameters that disturb the object localization problem, are the noise, the lack of knowledge of the scattering model and the presence of correlated signals. In the literature there is any method able to solve all those parameters. However we can found a satisfying method to cope with each parameter (noise,

correlated signals and lack of knowledge of the scattering model) alone, thus we have selected the following methods,

- High order statistics are famous by their power to remove the additive Gaussian noise and then to clean the data. It consists in using the slice cumulant matrix instead of using the spectral matrix and operate at a fixed frequency (narrowband signal). It has been employed in the MUSIC method in order to estimate the bearing sources (Gönen & Mendel, 1997), (Mendel, 1991),

- The frequential smoothing is a technique which allows us to decorrelate the wideband signals (Valaee & Kabal, 1995) by means of an average of the focused spectral matrices formed for all the frequencies of the frequency band. It has been employed also in the MUSIC method in order to estimate the bearing sources,

- The exact solution of the acoustic scattering model has been addressed in many published work for several configurations, as single (Doolittle & Uberall, 1966),
  (Goodman & Stern, 1962) or multiple objects (Prada & Fink, 1998), (Zhen, 2001), buried or partially buried objects (Lim et al., 1993), (Tesei et al., 2002), with cylindrical (Doolittle & Uberall, 1966), (Junger, 1952), or spherical shape (Fawcett et al., 1998), (Goodman & Stern, 1962), (Junger, 1952),

In this chapter we propose to adapt array processing methods and acoustic scattering model listed above in order to solve the problem of burried object with known shape by estimating their bearing and range, considering wideband correlated signals in presence of Gaussian noise. The fourth-order cumulant matrix (Gönen & Mendel, 1997), (Mendel, 1991) is used instead of the cross-spectral matrix to remove the additive Gaussian noise. The bilinear focusing operator is used to decorrelate the signals (Valaee & Kabal, 1995) and to estimate the coherent signal subspace (Valaee & Kabal, 1995), (Wang & Kaveh, 1985). From the exact solution of the acoustic scattered field (Fawcett et al., 1998), (Junger, 1952), we have derived a new source steering vector including both the range and the bearing objects. This source steering vector is employed in MUSIC (MUltiple SIgnal Classification) algorithm (Valaee & Kabal, 1995) instead of the classical plane wave model.

The organization of this chapter is as follows : the problem is formulated in Section 2. In Section 3, the scattering models are presented. In Section 4, the cumulant based coherent signal subspace method for bearing and range estimation is presented. Experimental setup and the obtained results supporting our conclusions and demonstrating our method are provided in Sections 5 and 6. Finally, conclusions are presented in Section 7.

Throughout the chapter, lowercase boldface letters represent vectors, uppercase boldface letters represent matrices, and lower and uppercase letters represent scalars. The symbol "T" is used for transpose operation, the superscript "+" is used to denote complex conjugate transpose, the subscript "*" is used to denote conjugate operation, and $||.||$ denotes the L_2 norm for complex vectors.

2. Problem formulation

We consider a linear array of N sensors which received the wideband signals scattered from P objects ($N > P$) in the presence of an additive Gaussian noise. The received signal vector, in

the frequency domain, is given by (Gönen & Mendel, 1997), (Mendel, 1991)

$$\mathbf{r}(f_n) = \mathbf{A}(f_n)\mathbf{s}(f_n) + \mathbf{b}(f_n), \text{ for } n = 1, ..., L \quad (1)$$

where,

$$\mathbf{A}(f_n) = [\mathbf{a}(f_n, \theta_1, \rho_1), \mathbf{a}(f_n, \theta_2, \rho_2), ..., \mathbf{a}(f_n, \theta_P, \rho_P)], \quad (2)$$

$$\mathbf{s}(f_n) = [s_1(f_n), s_2(f_n), ..., s_P(f_n)]^T, \quad (3)$$

$$\mathbf{b}(f_n) = [b_1(f_n), b_2(f_n), ..., b_N(f_n)]^T. \quad (4)$$

$\mathbf{r}(f_n)$ is the Fourier transforms of the array output vector, $\mathbf{s}(f_n)$ is the vector of zero-mean complex random non-Gaussian source signals, assumed to be stationary over the observation interval, $\mathbf{b}(f_n)$ is the vector of zero-mean complex white Gaussian noise and statistically independent of signals and $\mathbf{A}(f_n)$ is the transfer matrix (steering matrix) of the source sensor array systems computed by the $\mathbf{a}(f_n, \theta_k, \rho_k)$ for $k = 1, ..., P$, object steering vectors, assumed to have full column rank, it is given by:

$$\mathbf{a}(f_n, \theta_k, \rho_k) = [a(f_n, \theta_{k1}, \rho_{k1}), a(f_n, \theta_{k2}, \rho_{k2}), ..., a(f_n, \theta_{kN}, \rho_{kN})]^T, \quad (5)$$

where θ_k and ρ_k are the bearing and the range of the kth object to the first sensor of the array, thus, $\theta_k = \theta_{k1}$ and $\rho_k = \rho_{k1}$. In addition to the model equation (1), we also assume that the signals are statistically independent. In this case, a fourth order cumulant is given by

$$\text{Cum}(r_{k_1}, r_{k_2}, r_{l_1}, r_{l_2}) = \text{E}\{r_{k_1} r_{k_2} r_{l_1}^* r_{l_2}^*\} - \text{E}\{r_{k_1} r_{l_1}^*\}\text{E}\{r_{k_2} r_{l_2}^*\} - \text{E}\{r_{k_1} r_{l_2}^*\}\text{E}\{r_{k_2} r_{l_1}^*\}$$

where r_{k_1} is the k_1 element in the vector $\mathbf{r}$ and where $\text{E}[.]$ denotes the expectation operator. The indices k_1, k_2, l_1, l_2 are similarly defined. The cumulant matrix consisting of all possible permutations of the four indices $\{k_1, k_2, l_1, l_2\}$ is given in (Yuen & Friedlander, 1997) as

$$\mathbf{C}(f_n) = \sum_{k=1}^{P} \left(\mathbf{a}(f_n, \theta_k, \rho_k) \otimes \mathbf{a}^*(f_n, \theta_k, \rho_k)\right) u_k(f_n) \left(\mathbf{a}(f_n, \theta_k, \rho_k) \otimes \mathbf{a}^*(f_n, \theta_k, \rho_k)\right)^+ \quad (6)$$

where $u_k(f_n)$ is the source kurtosis (i.e., fourth order analog of variance) defined by

$$u_k(f_n) = \text{Cum}(s_k(f_n), s_k^*(f_n), s_k(f_n), s_k^*(f_n)) \quad (7)$$

of the kth complex amplitude source and $\otimes$ is the Kronecker product. When there are N array sensors, $\mathbf{C}(f_n)$ is $(N^2 \times N^2)$ matrix. The rows of $\mathbf{C}(f_n)$ are indexed by $(k_1 - 1)N + l_1$, and the columns are indexed by $(l_2 - 1)N + k_2$. In terms of the vector $\mathbf{r}(f_n)$, the cumulant matrix $\mathbf{C}(f_n)$ is organized compatibly with the matrix, $\text{E}\{(\mathbf{r}(f_n) \otimes \mathbf{r}^*(f_n))(\mathbf{r}(f_n) \otimes \mathbf{r}^*(f_n))^+\}$. In other words, the elements of $\mathbf{C}(f_n)$ are given by:

$$\mathbf{C}((k_1 - 1)N + l_1, (l_2 - 1)N + k_2) \quad (8)$$

for $k_1, k_2, l_1, l_2 = 1, 2, ..., N$ and

$$\mathbf{C}\big((k_1 - 1)N + l_1, (l_2 - 1)N + k_2\big) = \mathrm{Cum}(r_{k_1}, r_{k_2}, r_{l_1}, r_{l_2}) \tag{9}$$

where r_i is the ith element of the vector $\mathbf{r}$. In order to reduce the calculating time, instead of using the cumulant matrix $\mathbf{C}(f_n)$, a cumulant slice matrix $(N \times N)$ of the observation vector at frequency f_n can be calculated and it offers the same algebraic properties of $\mathbf{C}(f_n)$. This matrix is denoted $\mathbf{C}_1(f_n)$ (Gönen & Mendel, 1997), (Yuen & Friedlander, 1997). If we consider a cumulant slice, for example, by using the first row of $\mathbf{C}(f_n)$ and reshape it into an $(N \times N)$ hermitian matrix (Bourennane & Bendjama, 2002), i.e.

$$\mathbf{C}_1(f_n) = \mathrm{Cum}\big(r_1(f_n), r_1^*(f_n), \mathbf{r}(f_n), \mathbf{r}^+(f_n)\big)$$

$$= \begin{bmatrix} c_{1,1} & c_{1,N+1} & \cdots & c_{1,N^2-N+1} \\ c_{1,2} & c_{1,N+2} & \cdots & c_{1,N^2-N+2} \\ \vdots & \vdots & \vdots & \vdots \\ c_{1,N} & c_{1,2N} & \cdots & c_{1,N^2} \end{bmatrix}$$

$$= \mathbf{A}(f_n)\mathbf{U}_s(f_n)\mathbf{A}^+(f_n) \tag{10}$$

where $c_{1,j}$ is the $(1, j)$ element of the cumulant matrix $\mathbf{C}(f_n)$ and $\mathbf{U}_s(f_n)$ is the diagonal kurtosis matrix, its ith element is defined as, $\mathrm{Cum}\big(s_i(f_n), s_i^*(f_n), s_i(f_n), s_i^*(f_n)\big)$ with $i = 1, ..., P$. $\mathbf{C}_1(f_n)$ can be reported as the classical covariance or spectral matrix of received data

$$\mathbf{\Gamma}_r(f_n) = \mathrm{E}\big[\mathbf{r}(f_n)\mathbf{r}^+(f_n)\big] = \mathbf{A}(f_n)\mathbf{\Gamma}_s(f_n)\mathbf{A}^+(f_n) + \mathbf{\Gamma}_b(f_n) \tag{11}$$

where $\mathbf{\Gamma}_b(f_n) = \mathrm{E}\big[\mathbf{b}(f_n)\mathbf{b}^+(f_n)\big]$ is the spectral matrix of the noise vector and

$$\mathbf{\Gamma}_s(f_n) = \mathrm{E}\big[\mathbf{s}(f_n)\mathbf{s}^+(f_n)\big] \tag{12}$$

is the spectral matrix of the complex amplitudes $\mathbf{s}(f_n)$.
If the noise is white then:

$$\mathbf{\Gamma}_b(f_n) = \sigma_b^2(f_n)\mathbf{I}, \tag{13}$$

where $\sigma_b^2(f_n)$ is the noise power and $\mathbf{I}$ is the $(N \times N)$ identity matrix. The signal subspace is shown to be spanned by the P eigenvectors corresponding to P largest eigenvalues of the data spectral matrix $\mathbf{\Gamma}_r(f_n)$. But in practice, the noise is not often white or its spatial structure is unknown, hence the interest of the high order statistics as shown in equation (4) in which the fourth order cumulants are not affected by additive Gaussian noise (i.e., $\mathbf{\Gamma}_b(f_n) = 0$), so as no noise spatial structure assumption is necessary. If the eigenvalues and the corresponding eigenvectors of $\mathbf{C}_1(f_n)$ are denoted by $\{\lambda_i(f_n)\}_{i=1..N}$ and $\{\mathbf{v}_i(f_n)\}_{i=1..N}$. Then, the eigendecomposition of the cumulant matrix $\mathbf{C}_1(f_n)$ is exploited so as

$$\mathbf{C}_1(f_n) = \sum_{i=1}^{N} \lambda_i(f_n)\mathbf{v}_i(f_n)\mathbf{v}_i^+(f_n) \tag{14}$$

In matrix representation, equation (14) can be written

$$\mathbf{C}_1(f_n) = \mathbf{V}(f_n)\Lambda(f_n)\mathbf{V}^+(f_n) \tag{15}$$

where

$$\mathbf{V}(f_n) = [\mathbf{v}_1(f_n),...,\mathbf{v}_N(f_n)] \tag{16}$$

and

$$\Lambda(f_n) = diag(\lambda_1(f_n),...,\lambda_N(f_n)). \tag{17}$$

Assuming that the columns of $\mathbf{A}(f_n)$ are all different and linearly independent it follows that for nonsingular $\mathbf{C}_1(f_n)$, the rank of $\mathbf{A}(f_n)\mathbf{U}_s(f_n)\mathbf{A}^+(f_n)$ is P. This rank property implies that:

- the $(N - P)$ multiplicity of its smallest eigenvalues : $\lambda_{P+1}(f_n) = \ldots = \lambda_N(f_n) \cong 0$.

- the eigenvectors $\mathbf{V}_b(f_n) = \{\mathbf{v}_{P+1}(f_n)\ldots\mathbf{v}_N(f_n)\}$ corresponding to the minimal eigenvalues are orthogonal to the columns of the matrix $\mathbf{A}(f_n)$, namely, the steering vectors of the signals

$\mathbf{V}_b(f_n) = \{\mathbf{v}_{P+1}(f_n)\ldots\mathbf{v}_N(f_n)\}\perp\{\mathbf{a}(f_n,\theta_1,\rho_1)\ldots\mathbf{a}(f_n,\theta_P,\rho_P)\}$

The eigenstructure based techniques are based on the exploitation of these properties. The spatial spectrum of the conventional MUSIC method can be modified as follows in order to estimate both the range and the bearing of objects at the frequency f_n,

$$Z(f_n,\theta_k,\rho_k) = \frac{1}{\mathbf{a}^+(f_n,\theta_k,\rho_k)\mathbf{V}_b(f_n)\mathbf{V}_b^+(f_n)\mathbf{a}(f_n,\theta_k,\rho_k)} \tag{18}$$

Then the location (θ_k,ρ_k) for $k = 1,...,P$, maximizing the modified MUSIC spectrum in (18) is selected as the estimated object center to the first sensor of the array. Because a two dimensional search requires that the exact solution of the scattered field be calculated at each point in order to fill the steering vector $\mathbf{a}(f_n,\theta_k,\rho_k)$.

3. The scattering model

In this section we present how to fill the steering vector used in equation (18) at a fixed frequency f_n. Consider the case in which a plane wave is incident, with an angle θ_{inc}, on P infinite elastic cylindrical shells or elastic spherical shells of inner radius β_k and outer radius α_k for $k = 1,...,P$, located in a free space at (θ_k,ρ_k) the bearing and the range of the *kth* object, associated to the first sensor of the array $\mathbf{S}_1$ (see figure 1). The fluid outside the shells is labeled by 1, thus, the sound velocity c_1 and the wavenumber

$$K_{n1} = \frac{2\pi f_n}{c_1}.$$

3.1 Cylindrical shell

We consider the case of infinitely long cylindrical shell. In order to calculate the exact solution for the acoustic scattered field $a_{cyl}(f_n,\theta_{k1},\rho_{k1})$ a decomposition of the different fields is used, according to the Bessel functions J_m, N_m and the Hankel function (H_m).

The scattered pressure in this case is given by (Doolittle & Uberall, 1966),(Junger, 1952),

$$a_{cyl}(f_n, \theta_{k1}, \rho_{k1}) = p_{c0} \sum_{m=0}^{\infty} j^m \epsilon_m b_m H_m^{(1)}(K_{n1}\rho_{k1}) \cos(m(\theta_{k1} - \theta_{inc})), \tag{19}$$

where p_{c0} is a constant, $\epsilon_0 = 1, \epsilon_1 = \epsilon_2 = ... = 2$, b_m is a coefficient depending on conditions limits and m is the number of modes (Doolittle & Uberall, 1966).

3.2 Spherical shell

The analysis is now extended to the case where the scatterer is a spherical shell. The scattered pressure is given by (Fawcett et al., 1998), (Goodman & Stern, 1962), (Junger, 1952)

$$a_{sph}(f_n, \theta_{k1}, \rho_{k1}) = p_{s0} \sum_{m=0}^{\infty} B_m H_m^{(1)}(K_{n1}\rho_{k1}) P_m(\cos(\theta_{k1} - \theta_{inc})), \tag{20}$$

where p_{s0} is a constant and $P_m(\cos(\theta_{k1} - \theta_{inc}))$ is the Legendre polynomials (Goodman & Stern, 1962). Equations (19) and (20) give the first component of the steering vector, then, in a similar manner the other component $a_{cyl}(f_n, \theta_{ki}, \rho_{ki})$ and $a_{sph}(f_n, \theta_{ki}, \rho_{ki})$ for $i = 2, ..., N$, associated to the *ith* sensor, can be formed, where all the couples (θ_{ki}, ρ_{ki}) are calculated using the general Pythagore theorem and are function of the couple (θ_{k1}, ρ_{k1}). Thus, the configuration used is shown in figure 1. The obtained θ_{ki}, ρ_{ki} are given by

$$\rho_{ki} = \sqrt{\rho_{ki-1}^2 - d^2 - 2\rho_{ki-1}d\cos(\frac{\pi}{2} + \theta_{ki-1})} \tag{21}$$

$$\theta_{ki} = \cos^{-1}[\frac{d^2 + \rho_{ki}^2 - \rho_{ki-1}^2}{2\rho_{ki-1}d}], \tag{22}$$

where d is the distance between two adjacent sensors. Finally the steering vector is filled with the cylindrical scattering model in the case of cylindrical shells and filled with the spherical scattering model in the case of spherical shells. For example, when the considered objects are cylindrical shells, the steering vector is written as:

$$\mathbf{a}(f_n, \theta_k, \rho_k) = \left[a_{cyl}(f_n, \theta_{k1}, \rho_{k1}), ..., a_{cyl}(f_n, \theta_{kN}, \rho_{kN}) \right]^T, \tag{23}$$

By using the exact solution of the scattered field (Doolittle & Uberall, 1966), we can fill the direction vector in the MUSIC algorithm equation (18) with non planar scattered field to locate the objects. The location $(\hat{\rho}, \hat{\theta})$ maximizing the MUSIC spectrum in (18) is selected as the estimated object center.

Because a two dimensional search requires that the exact scattered field be calculated at each point. The modified MUSIC algorithm presented in this section, is limited to one or multiple objects localization where the interactions are ignored. So, the localization problem is approached as if these objects are independently scattering the incident plane wave.
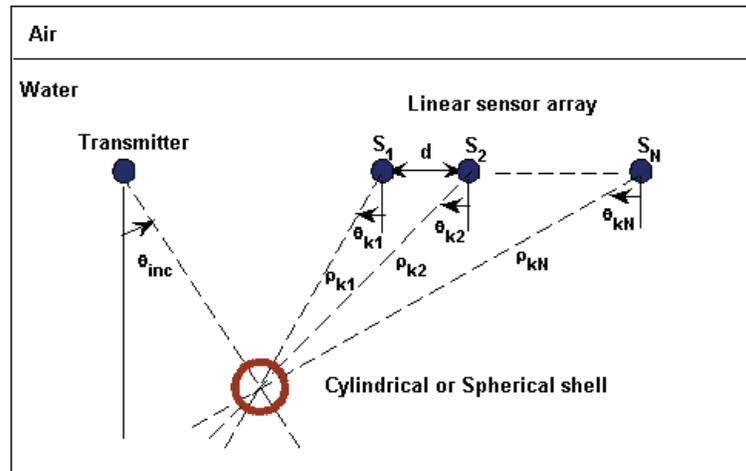
Fig. 1. Geometry configuration of the *kth* object localization.

4. The cumulant based coherent signal subspace method for bearing and range estimation

In the previous section, a modified MUSIC algorithm has been proposed in order to estimate both the range and the bearing objects at a fixed frequency. In this section, the frequency diversity of wideband signals is considered. The received signals come from the reflections on the buried objects thus these signals are totally correlated and the MUSIC method looses its performances if any preprocessing is used before as the spatial smoothing (Pillai & Kwon, 1989) or the frequential smoothing (Frikel & Bourennane, 1996), (Valaee & Kabal, 1995). It appears clearly that it is necessary to apply any preprocessing to decorrelate the signals. According to the published results (Pillai & Kwon, 1989), the spatial smoothing needs a greater number of sensors than the frequential smoothing.

In this section, the employed signals are wideband. This choice is made in order to decorrelate the signals by means of an average of the focused spectral matrices. Therefore the objects can be localized even if the received signals are totally correlated. This would have not been possible with the narrowband signals without the spatial smoothing. Among the frequential smoothing based processing framework (Maheswara & Reddy, 1996), (Pillai & Kwon, 1989), we have chosen the optimal method which is the bilinear focusing operator (Frikel & Bourennane, 1996), (Valaee & Kabal, 1995), in order to obtain the coherent signal subspace. This technique divides the frequency band into L narrowbands (Frikel & Bourennane, 1996), (Valaee & Kabal, 1995), then, transforms the received signals in the L bands into the focusing frequency f_0. The average of the focused signals is then calculated and consequently decorrelates the signals (Hung & Kaveh, 1988), (Wang & Kaveh, 1985). Here, f_0 is the center frequency of the spectrum of the received signal and it is chosen as the focusing frequency. The following is the step-by-step description of the technique:

1. use an ordinary beamformer to find an initial estimate of P, θ_k and ρ_k for $k = 1, ..., P$,

2. fill the transfer matrix,

$$\hat{\mathbf{A}}(f_n) = [\mathbf{a}(f_n, \theta_1, \rho_1), \mathbf{a}(f_n, \theta_2, \rho_2), ..., \mathbf{a}(f_n, \theta_P, \rho_P)], \tag{24}$$

where each component of the directional vector $\mathbf{a}(f_n, \theta_k, \rho_k)$ for $k = 1, ..., P$, is filled using equation (19) or (20) considering the object shape,

3. estimate the cumulant slice matrix output sensors data $\mathbf{C}_1(f_n)$ at frequency f_n,

4. calculate object cumulant matrix at each frequency f_n using equation (10):

$$\mathbf{U}_s(f_n) = (\hat{\mathbf{A}}^+(f_n)\hat{\mathbf{A}}(f_n))^{-1}\hat{\mathbf{A}}^+(f_n)[\mathbf{C}_1(f_n)]\hat{\mathbf{A}}(f_n)(\hat{\mathbf{A}}^+(f_n)\hat{\mathbf{A}}(f_n))^{-1}, \tag{25}$$

5. calculate the average of the cumulant matrices associated to the objects,

$$\bar{\mathbf{U}}_s(f_0) = \frac{1}{L}\sum_{n=1}^{L}\mathbf{U}_s(f_n), \tag{26}$$

6. calculate $\hat{\mathbf{C}}_1(f_0) = \hat{\mathbf{A}}(f_0)\bar{\mathbf{U}}_s(f_0)\hat{\mathbf{A}}^+(f_0)$

7. form the focusing operator using the eigenvectors,

$$\mathbf{T}(f_0, f_n) = \hat{\mathbf{V}}_s(f_0)\mathbf{V}_s^+(f_n) \tag{27}$$

where $\mathbf{V}_s(f_n)$ and $\hat{\mathbf{V}}_s(f_0)$ are the eigenvectors associated with the largest eigenvalues of the cumulant matrix $\mathbf{C}_1(f_n)$ and $\hat{\mathbf{C}}_1(f_0)$, respectively.

8. form the average slice cumulant matrix $\bar{\mathbf{C}}_1(f_0)$ and perform its eigendecomposition,

$$\bar{\mathbf{C}}_1(f_0) = \frac{1}{L}\sum_{n=1}^{L}\mathbf{T}(f_0, f_n)\mathbf{C}_1(f_n)\mathbf{T}^+(f_0, f_n) \tag{28}$$

The modified spatial spectrum of MUSIC method for wideband correlated signals is given by

$$Z_{wb}(f_0, \theta_k, \rho_k) = \frac{1}{\mathbf{a}^+(f_0, \theta_k, \rho_k)\bar{\mathbf{V}}_b(f_0)\bar{\mathbf{V}}_b^+(f_0)\mathbf{a}(f_0, \theta_k, \rho_k)}, \tag{29}$$

where $\bar{\mathbf{V}}_b(f_0)$ is the eigenvector matrix of $\bar{\mathbf{C}}_1(f_0)$ associated to the smallest eigenvalues.

5. Experimental setup

An underwater acoustic data have been recorded in an experimental water tank (figure 2) in order to evaluate the performances of the developed method. This tank is fill of water and homogeneous fine sand, where are buried three cylinder couples and one sphere couple, full of water or air, between 0 and 0.005 m, of different dimensions (see table 1). The considered sand has geoacoustic characteristics near to those of water. Consequently, we can make the assumption that the objects are in a free space. The experimental setup is shown in figure 3 where all the dimensions are given in meter. The considered cylindrical and spherical shells are made of dural aluminum with density $D_2 = 1800$ kg/m^3, the longitudinal and transverse-elastic wave velocities inside the shell medium are $c_l = 6300$ m/s and $c_t = 3200$
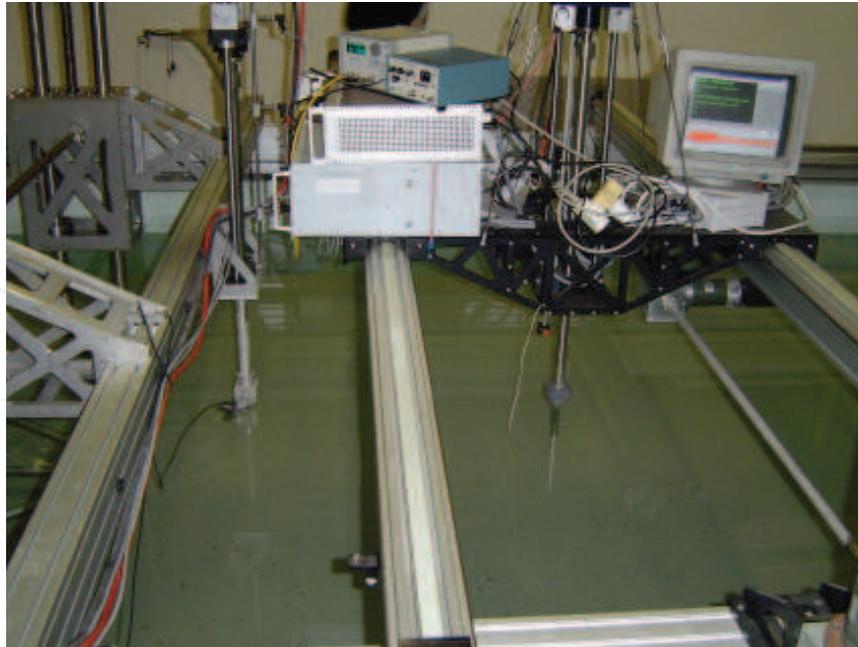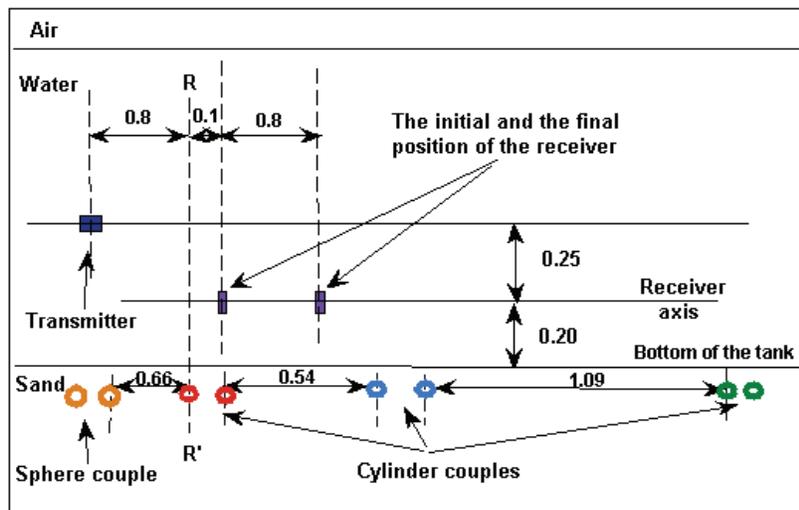
Fig. 2. Experimental tank

Fig. 3. Experimental setup

m/s, respectively. The external fluid is water with density $D_1 = 1000$ kg/m^3 and the the internal fluid is water or air with density $D_{3air} = 1.2\ 10^{-6}$ kg/m^3 or $D_{3water} = 1000$ kg/m^3. We have done eight experiments where the transmitter is fixed at an incident angle $\theta_{inc} = 60°$ and the receiver moves horizontally, step by step, from the initial to the final position with a step size $d = 0.002$ m and takes 10 positions in order to form an array of sensors with $N = 10$. The distance, between the transmitter, the RR' axis and the receiver, remains the same. First time, we have fixed the receiver horizontal axis at 0.2 m from the bottom of the tank, then, we have done four experiments, Exp. 1, Exp. 2, Exp. 3 and Exp. 4, associated to the following

	1st couple	2nd couple
Outer radius α_k (m)	$\alpha_{1,2} = 0.30$	$\alpha_{3,4} = 0.01$
Filled of	air	air
Separated by (m)	0.33	0.13

	3rd couple	4th couple
Outer radius α_k (m)	$\alpha_{5,6} = 0.018$	$\alpha_{7,8} = 0.02$
Filled of	water	air
Separated by (m)	0.16	0.06

Table 1. characteristics of the various objects (the inner radius $\beta_k = \alpha_k - 0.001$ m, for $k = 1, ..., P$)

configuration; the RR' axis is positioned on the sphere couple, the 1st, the 2nd and the 3rd cylinder couple, respectively. Second time, the receiver horizontal axis is fixed at 0.4 m and in the same manner we have done four other experiments Exp. 5, Exp. 6, Exp. 7 and Exp. 8 associated to each position of the RR'. Thus, for each experiment, only one object couple is radiated by the transmitter, where the transmitted signal has the following properties; impulse duration is 15 μs, the frequency band is $[f_L = 150, f_U = 250]$ kHz, the mid-band frequency is $f_0 = 200$ kHz and the sampling rate is 2 MHz. The duration of the received signal is 700 μs.

5.1 Experimental data

At each sensor, time-domain data is collected and the typical sensor output signals corresponding to one experiment are shown in figure 4. The power spectral density of the sensor output signal is presented in figure 5.
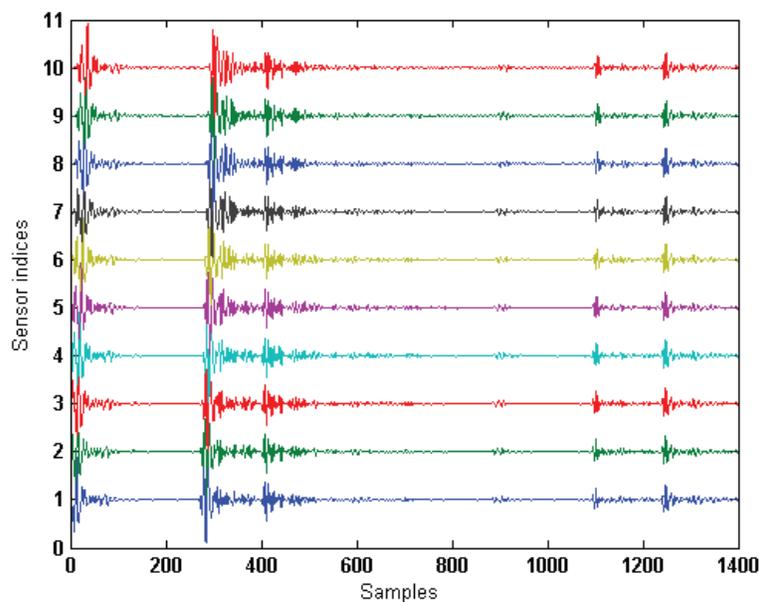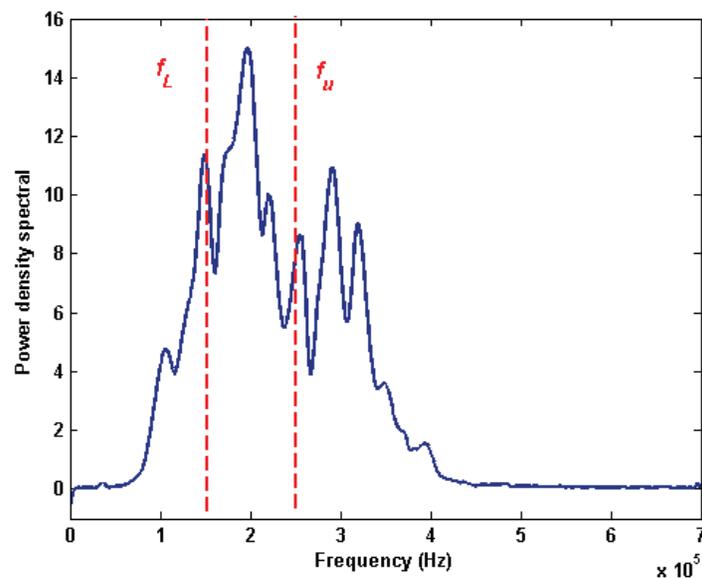

Fig. 4. Observed sensor output signals

Fig. 5. Power spectral density of sensor output signal.

6. Results and discussion

The steps listed above in section 4, are applied on each experimental data, thus, an initialization of θ, ρ and P has been done using the conventional beamformer and for example for Exp. 1, those three parameters have been initialized by $P = 1$, $\theta_1 = 15°$ and $\rho_1 = 0.28$ m. Moreover, the average of the focused slice cumulant matrices is calculated using $L = 50$ frequencies chosen in the frequency band of interest $[f_L, f_U]$. Moreover, a sweeping on the bearing and the range have been applied ($[-90°, 90°]$ for the bearing with a step $0.1°$ and $[0.2, 1.5]$ m for the range with a step 0.002 m). The obtained spatial spectrum of the modified MUSIC method are shown in figures 6 to 13. On each figure, we should have two peaks associated to one object couple and that is what appears on the majority of figures.

Table 2 summarizes the expected and the estimated range and bearing objects obtained using the MUSIC algorithm alone, then using the modified MUSIC algorithm with and without a frequential smoothing. The indexes 1 and 2 are the 1st and the 2nd object of each couple of cylinders or spheres. Note that the obtained bearing objects after applying the conventional MUSIC algorithm are not exploitable. Similar results are obtained when we apply the modified MUSIC algorithm without a frequential smoothing, because the received signals are correlated due to the small distance that separate the objects each other and the use of a single transmitter sensor. However, satisfying results are obtained when we apply the modified MUSIC algorithm with a frequential smoothing, thus the majority of bearing and range objects are successfully estimated. Furthermore, the difference between the estimated value ($\theta_{(1,2)est}, \rho_{(1,2)est}$) and the expected value ($\theta_{(1,2)exp}, \rho_{(1,2)exp}$) is very small and only two cylinders were not detected in Exp. 6 and Exp. 8, because, the received echoes, associated to these cylinders, are rather weak. Thus, it is important to realize that there is some phenomenons which complicate the object detection in experimental tank, for example, the attenuation of high frequencies in sediment is much higher than the low frequencies and due to the small dimensions of the experimental tank, the frequencies used here are $[150, 250]$ kHz which represent high frequencies.
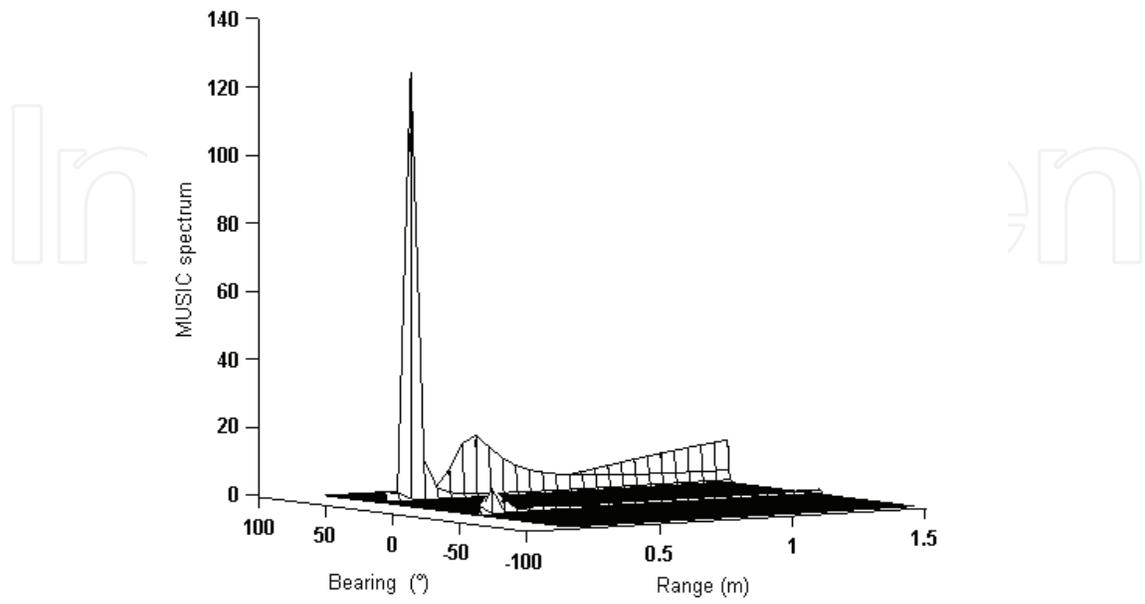
Fig. 6. Spatial spectrum of the developed method for air sphere couple (Exp.1.).
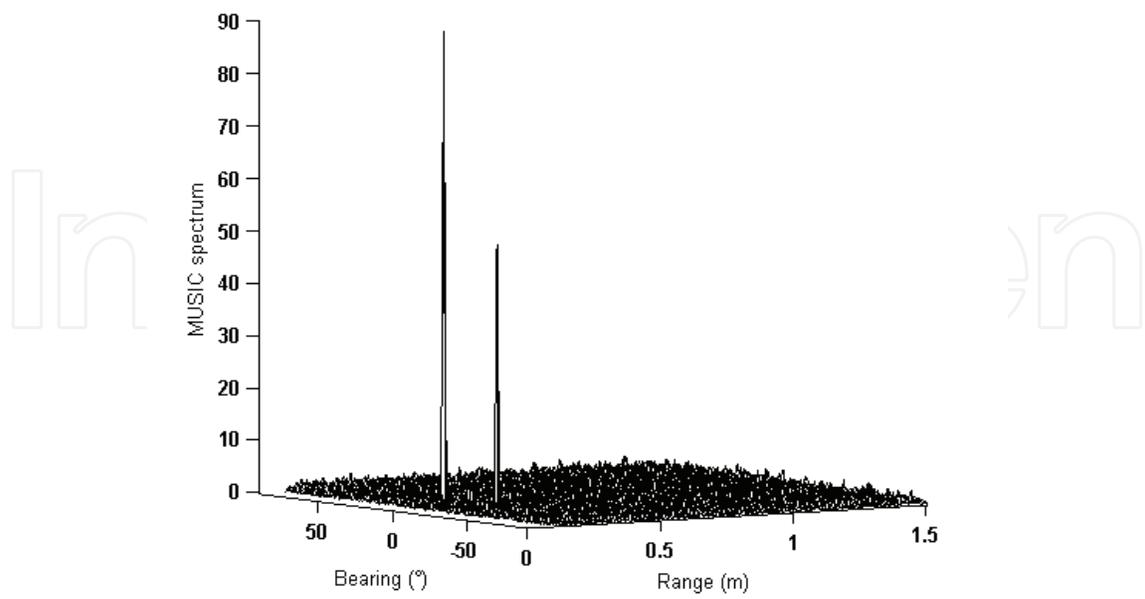

Fig. 7. Spatial spectrum of the developed method for small air cylinders couple (Exp.2).
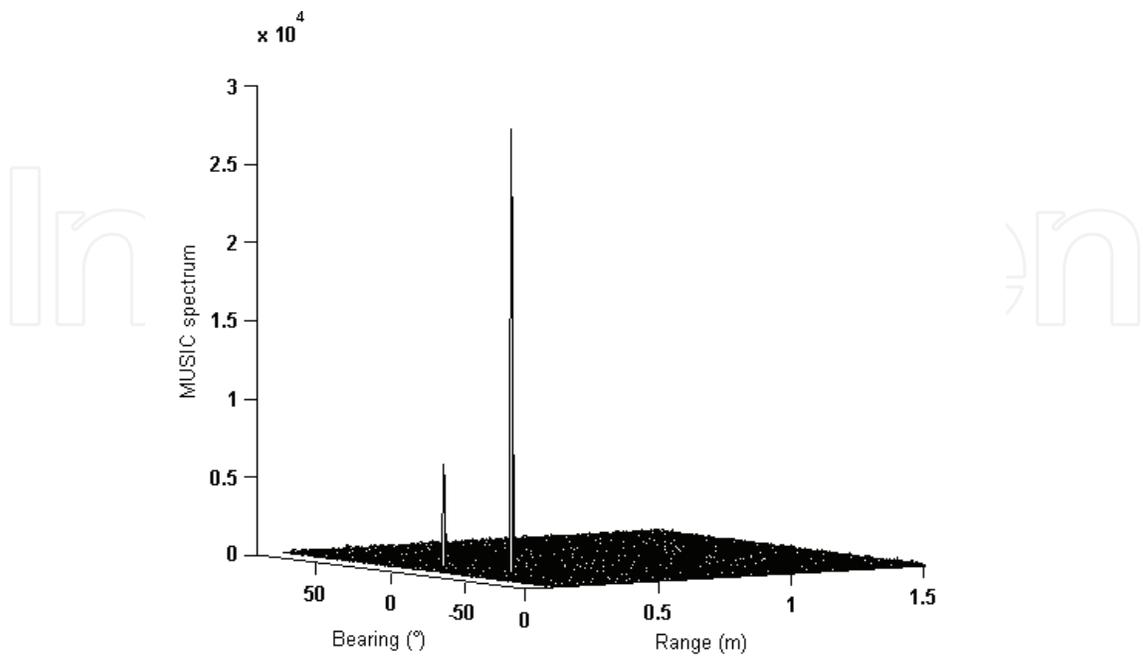
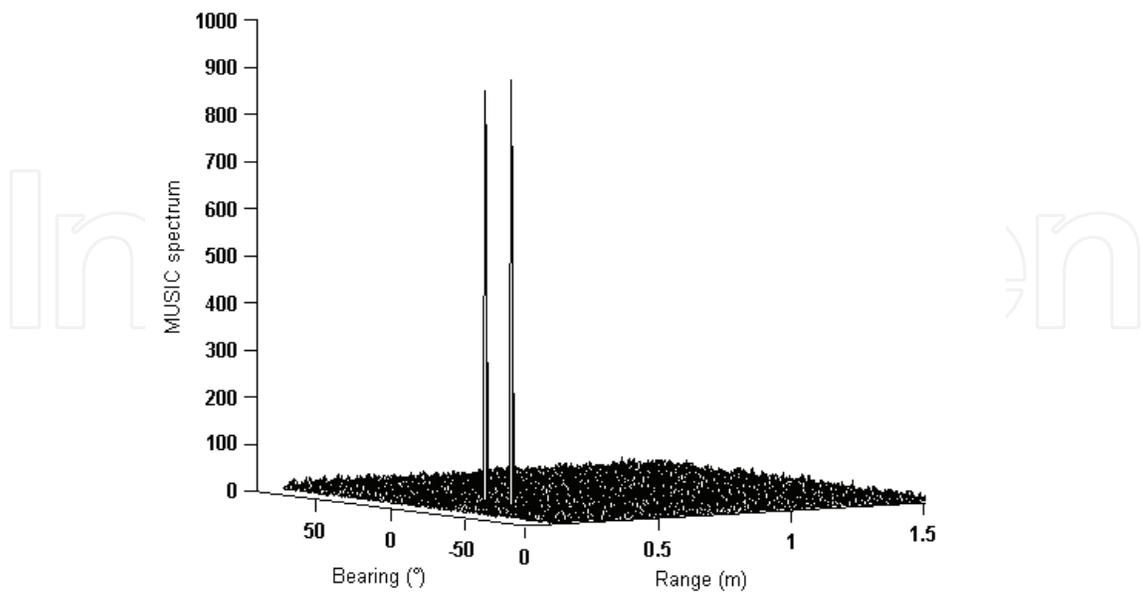Fig. 8. Spatial spectrum of the developed method for big water cylinders couple (Exp.3).

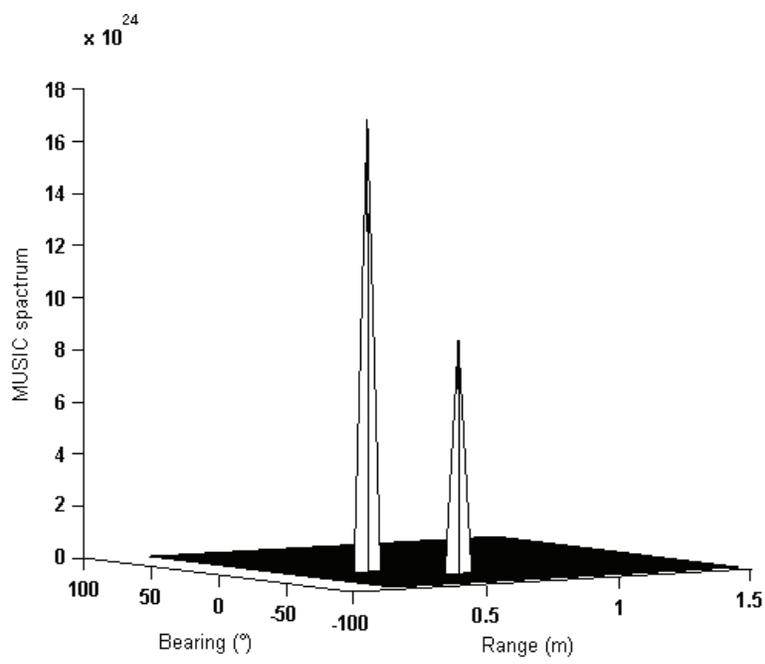Fig. 9. Spatial spectrum of the developed method for big air cylinders couple (Exp.4.).

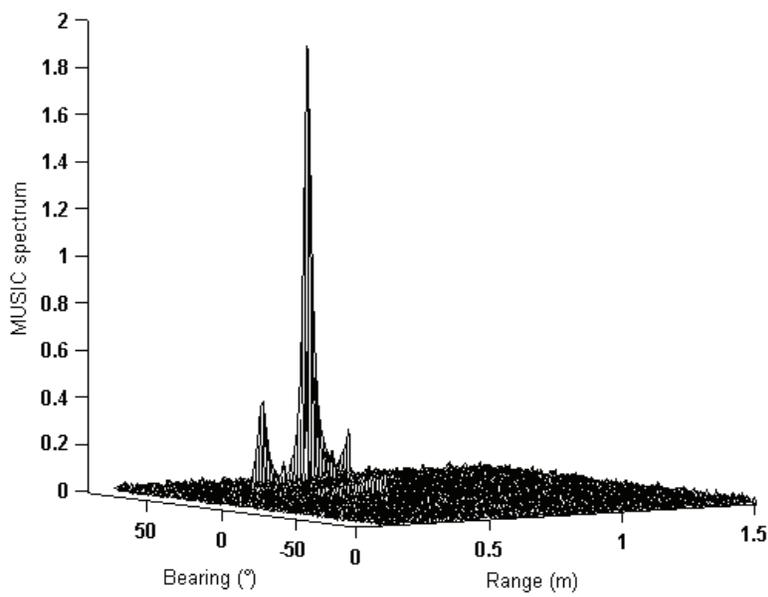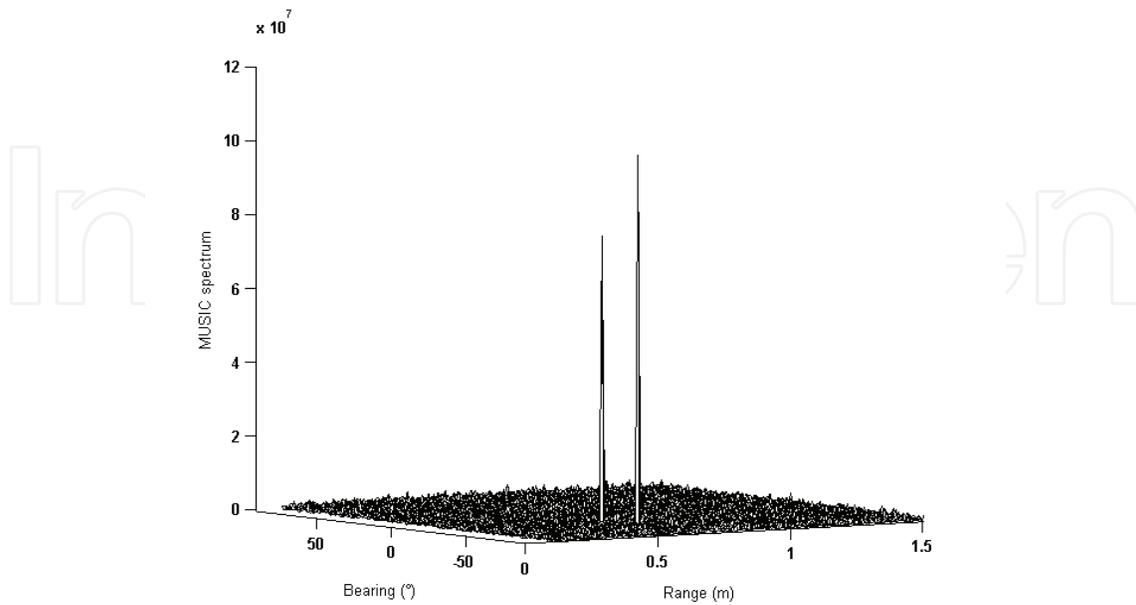Fig. 10. Spatial spectrum of the developed method for Air sphere couple (Exp.5.).

Fig. 11. Spatial spectrum of the developed method for small air cylinders couple (Exp.6).

Fig. 12. Spatial spectrum of the developed method for big water cylinders couple (Exp.7).
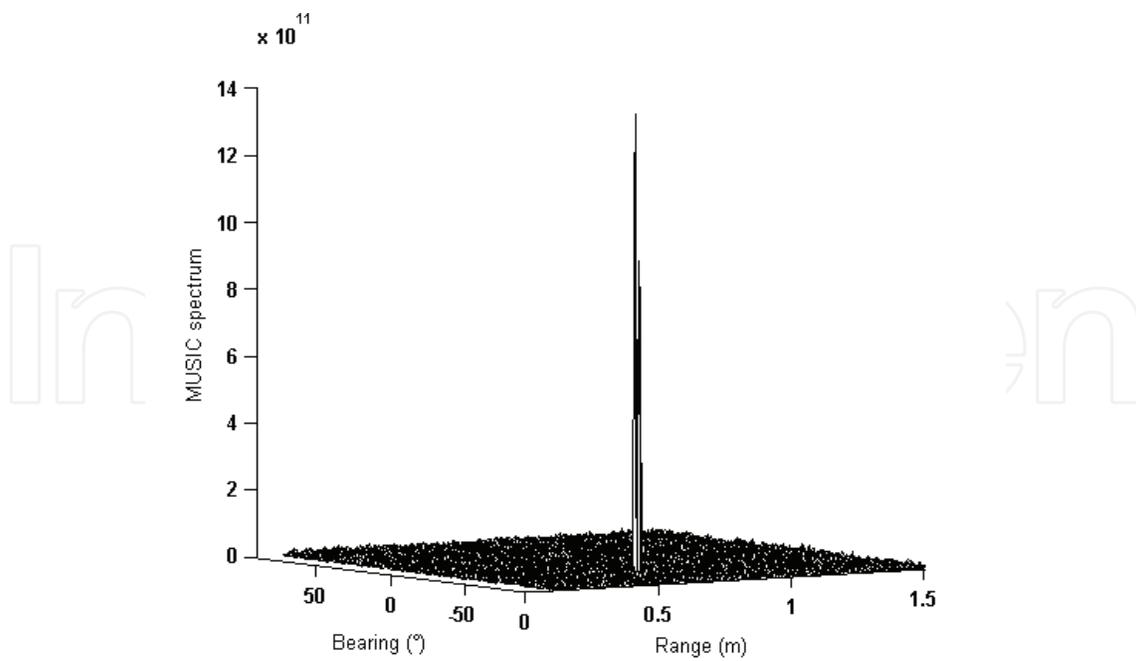

Fig. 13. Spatial spectrum of the developed method for big air cylinders couple (Exp.8.).

	Exp.1	Exp.2	Exp.3	Exp.4
$\theta_{1exp}(°)$	−26.5	−23	−33.2	−32.4
$\rho_{1exp}(m)$	0.24	0.24	0.26	0.26
$\theta_{2exp}(°)$	44	9.2	−20	5.8
$\rho_{2exp}(m)$	0.31	0.22	0.24	0.22
MUSIC				
$\theta_{1est}(°)$	−18	−30	−40	−22
$\theta_{2est}(°)$	30	−38	−48	−32
MUSIC NB				
$\theta_{1,2est}(°)$	15	−12	−28	−10
$\rho_{1,2est}(m)$	0.28	0.23	0.25	0.24
MUSIC WB				
$\theta_{1est}(°)$	−26	−23	−33	−32
$\rho_{1est}(m)$	0.22	0.25	0.29	0.28
$\theta_{2est}(°)$	43	9	−20	6
$\rho_{2est}(m)$	0.34	0.25	0.25	0.23

	Exp.5	Exp.6	Exp.7	Exp.8
$\theta_{1exp}(°)$	−50	−52.1	−70	−51.6
$\rho_{1exp}(m)$	0.65	0.65	1.24	0.65
$\theta_{2exp}(°)$	−22	−41	−65.3	−49
$\rho_{2exp}(m)$	0.45	0.56	1.17	0.64
MUSIC				
$\theta_{1est}(°)$	−58	25	−40	−
$\theta_{2est}(°)$	−12	−40	−45	−
MUSIC NB				
$\theta_{1,2est}(°)$	−35	−45	−70	−50
$\rho_{1,2est}(m)$	0.52	0.63	1.2	0.65
MUSIC WB				
$\theta_{1est}(°)$	−49	−52	−70	−52
$\rho_{1est}(m)$	0.65	0.63	1.21	0.63
$\theta_{2est}(°)$	−22	−	−65	−
$\rho_{2est}(m)$	0.44	−	1.2	−

Table 2. The expected (exp) and estimated (est) values of range and bearing objects. (negative bearing is clockwise from the vertical), NB: Narrowband, WB: Wideband)

7. Conclusion

In this chapter we have proposed a new method to estimate both the bearing and the range of buried objects in a noisy environment and in presence of correlated signals. To cope with the noise problem we have used high order statistics, thus we have formed the slice cumulant matrices at each frequency bin composed of clean data. Then, we have applied the coherent subspace method which consists in a frequential smoothing in order to cope with the signal correlation problem and to form the focusing slice cumulant matrix. To estimate the range and

the bearing objects, the focusing slice cumulant matrix is used instead of using the spectral matrix and the exact solution of the acoustic scattered field is used instead of the plane wave model, in the MUSIC method. We considered objects with known shapes as cylindrical or spherical shells, buried in an homogeneous sand. Our method can be applied when the objects are located in the nearfield and rather in the farfield region of the sensor array. The performances of this method are investigated through real data associated to many spherical and cylindrical shells buried under the sand. The proposed method is superior in terms of performance to the conventional method. The range and the bearing objects are estimated with a significantly good accuracy due to the free space assumption.

8. Acknowledgment

9. References

Granara, M.; Pescetto, A.; Repetto, F.; Tacconi, G. & Trucco, A. (1998). Statistical and neural techniques to buried object detection and classification. *Proceedings of OCEANS'98 Conference*, Vol. 3, pp. 1269-1273, Nice France, oct. 1998.

Nicq, G. & Brussieux, M. (1998). A time-frequency method for classifying objects at low frequencies. *Proc. OCEANS'98 conference*, Vol. 1, pp. 148-152, Nice France, oct. 1998.

Guillermin, R.; Lasaygues, P.; Sessarego, J.P. & Wirgin, A. (2000). Characterization of buried objects by a discretized domain integral equation inversion method using born approximation. *Proceedings of 5th Eur. Conf. Underwater Acoustics*, Vol. 2, pp. 863-868, Lyon France, july 2000.

Hetet, A.; Amate, M.; Zerr, B.; Legris, M.; Bellec, R.; Sabel, J.C. & Groen, J. (2004). SAS processing results for the detection of buried objects with a ship-mounted sonar. *Proceedings of the 7th Eur. Conf. Underwater Acoustics*, Delft Netherland, july 2004.

Roux, P. & Fink, M. (2000). Time-reversal in a waveguide: Study of the temporal and spatial focusing. *J. Acoust. Soc. Am.*, Vol. 107, No. 5, (2000) (2418-2429).

Gönen, E. & Mendel, J.M. (1997). Applications of cumulants to array processing - Part III : Blind beamforming for coherent signals. *IEEE Trans. on signal processing*, Vol. 45, No. 9, (1997) (2252-2264), ISSN 1053-587X.

Mendel, J.M. (1991). Tutorial on higher order statistics(spectra) in signal processing and system theory : Theoretical results and some applications. *Proceedings of the IEEE*, 1991, Vol. 79, No. 3, pp. 278-305, march 1991.

Valaee, S. & Kabal, P. (1995). Wideband array processing using a two-sided correlation transformation. *IEEE Trans. on signal processing*, Vol.43, No.1, (jan. 1995)(160-172), ISSN 1053-587X .

Doolittle, R. & Uberall, H. (1966). Sound scattering by elastic cylindrical shells. *J. Acoust. Soc. Am.*, Vol. 39, No. 2, (1966) (272-275), ISSN 0001-4966.

Goodman, R.& Stern, R. (1962). Reflection and transmission of sound by elastic spherical shells. *J. Acoust. Soc. Am.*, Vol. 34, No. 3, (march 1962) (338-344), ISSN 0001-4966 .

Prada, C. & Fink, M. (1998). Separation of interfering acoustic scattered signals using the invariants of the time reversal operator. Application to Lamb waves characterization. *J. Acoust. Soc. Am.*, Vol. 104, No. 2, (august 1998).

Zhen, Y. (2001). Recent developments in underwater acoustics: Acoustic scattering from single and multiple bodies. *Proc. Natl.Sci. Counc. ROC(A)*, Vol.25, No.3, (2001)(137-150).

Lim,R.; Lopes, J. L.; Hackman, R. H. & Todoroff, D. G.(1993). Scattering by objects buried in underwater sediments: Theory and experiment. *J. Acoust. Soc. Am.*, Vol. 93, No. 4, (april 1993).

Tesei, A.; Maguer, A. & Fox, W. L. J. (2002). Measurements and modeling of acoustic scattering from partially and completely buried spherical shells. *J. Acoust. Soc. Am.*, Vol. 112, No. 5, (november 2002).

Junger, M. C.(1952). Sound scattering by thin elastic shells. *J. Acoust. Soc. Am.*, Vol. 24, No. 4, (july 1952).

Fawcett,J.A.; Fox, W.L. & Maguer, A. (1998). Modeling by scattering by objects on the seabed. *J. Acoust. Soc. Am.*, Vol. 104, No. 6, (dec. 1998) (3296-3304), ISSN 0001-4966.

Wang, H. & Kaveh, M. (1985). Coherent signal-subspace processing for the detection and estimation of angles of arrival of multiple wide band sources. *IEEE Trans. on Acoustics, Speech and Signal Processing*, Vol. 33, No. 4, (aug. 1985) (823-831), ISSN 0096-3518.

Yuen, N. & Friedlander, B. (1997). DOA estimation in multipath : an approach using fourth order cumulants. *IEEE. Trans. on Signal Processing*, Vol. 45, No. 5, (may 1997) (1253-1263), ISSN 1053-587X .

Bourennane, S. & Bendjama, A. (2002). Locating wide band acoustic sources using higher-order statistics. *Applied Acoustics*, Vol. 63, No. 3, (march 2002) (235-251).

Pillai, S.& Kwon, B. (1989). Forward/Backward spatial smoothing techniques for coherent signal identification. *IEEE Trans. on Acoustics, Speech and Signal Processing*, Vol. 37, No. 1, (jan. 1989)(8-15), ISSN 0096-3518 .

Frikel, M. & Bourennane, S. (1996). Fast algorithm for the wideband array processing using two-sided correlation transformation. *Proceedings of EUSIPCO'96*, Vol. 2, pp. 959-962, Trieste Italy, Sept. 1996.

Maheswara Reddy, K.& Reddy, V.U. (1996). Further results in spatial smoothing. *Signal processing*, Vol. 48, (1996) (217-224).

Hung, H. & Kaveh, M. (1988). Focusing matrices for coherent signal-subspace processing. *IEEE Trans. on Acoustics, Speech and Signal Processing*, Vol. 36, No. 8, (Aug. 1988) (1272-1281), ISSN 0096-3518.
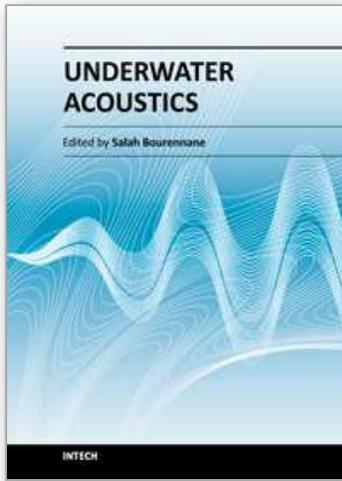
Underwater Acoustics

Edited by Prof. Salah Bourennane

How to reference

In order to correctly reference this scholarly work, feel free to copy and paste the following:

Caroline Fossati, Salah Bourennane and Julien Marot (2012). Localization of Buried Objects in Sediment Using High Resolution Array Processing Methods, Underwater Acoustics, Prof. Salah Bourennane (Ed.), ISBN: 978-953-51-0441-4, InTech, Available from: http://www.intechopen.com/books/underwater-acoustics/localization-of-buried-objects-in-sediment-using-high-resolution-array-processing-methods

INTECH
open science | open minds